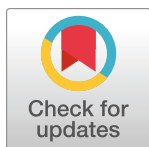# PLOS ONE

RESEARCH ARTICLE

NMR spectroscopy analysis reveals differential metabolic responses in arabidopsis roots and leaves treated with a cytokinesis inhibitor

Thomas E. Wilkop[1,2�‿], Minmin Wang[2�‿], Angelo Heringer[2], Jaideep Singh[3], Florence Zakharov[2], Viswanathan V. Krishnan[3,4]*, Georgia Drakakaki[2]*

1 Light Microscopy Core/ Department of Physiology, University of Kentucky, Lexington, KY, United States of America, 2 Department of Plant Sciences, University of California, Davis, CA, United States of America, 3 Department of Chemistry, California State University, Fresno, CA, United States of America, 4 Department of Medical Pathology and Laboratory Medicine, University of California School of Medicine, Sacramento, CA, United States of America

☿ These authors contributed equally to this work.
* krish@csufresno.edu, vvkrishnan@ucdavis.edu (VVK); gdrakakaki@ucdavis.edu (GD)

Abstract

In plant cytokinesis, *de novo* formation of a cell plate evolving into the new cell wall partitions the cytoplasm of the dividing cell. In our earlier chemical genomics studies, we identified and characterized the small molecule endosidin-7, that specifically inhibits callose deposition at the cell plate, arresting late-stage cytokinesis in arabidopsis. Endosidin-7 has emerged as a very valuable tool for dissecting this essential plant process. To gain insights regarding its mode of action and the effects of cytokinesis inhibition on the overall plant response, we investigated the effect of endosidin-7 through a nuclear magnetic resonance spectroscopy (NMR) metabolomics approach. In this case study, metabolomics profiles of arabidopsis leaf and root tissues were analyzed at different growth stages and endosidin-7 exposure levels. The results show leaf and root-specific metabolic profile changes and the effects of endosidin-7 treatment on these metabolomes. Statistical analyses indicated that the effect of endosidin-7 treatment was more significant than the developmental impact. The endosidin-7 induced metabolic profiles suggest compensations for cytokinesis inhibition in central metabolism pathways. This study further shows that long-term treatment of endosidin-7 profoundly changes, likely via alteration of hormonal regulation, the primary metabolism of arabidopsis seedlings. Hormonal pathway-changes are likely reflecting the plant's responses, compensating for the arrested cell division, which in turn are leading to global metabolite modulation. The presented NMR spectral data are made available through the Metabolomics Workbench, providing a reference resource for the scientific community.

Introduction

In a large-scale chemical genetics screening of small molecules interfering with endomembrane trafficking in arabidopsis [1], a number of highly specific compound-probes were identified. Among these compounds was endosidin-7, a heterocyclic organic molecule with attributes of both flavonoid and alkaloid derivatives (**Fig 1A**), that specifically inhibits callose deposition at the division plane, which consequently leads to late-stage cytokinesis arrest [2]. Cytokinesis is a fundamental process of all life on earth and is essential for plant growth and development. The tight regulation of this process involves the coordinated accumulation of membrane material and polysaccharide deposition. It is currently hypothesized that callose integration structurally stabilizes the maturing cell plate while it transitions into a new cell wall [3–5]. Cell plate formation involves highly orchestrated vesicle accumulation, fusion, and membrane network maturation, and is supported by the temporary integration of elastic and pliable callose [6, 7]. Currently, the integration and coordination of polysaccharide deposition, in conjunction with the membrane maturation during cell plate expansion, is ill-understood [6, 7]. A detailed understanding of the plant's metabolome in response to endosidin-7 treatment can provide insights into major metabolic fluxes during plant cytokinesis and potential compensating mechanisms to its inhibition.

The utility of endosidin-7 as a cytokinesis probe has been shown by its ability to reveal the interplay of specific vesicle populations during cell plate assembly [2, 8]. With the aid of endosidin-7, the timely pattern of vesicle contributions during cell plate expansion can be dissected to better understand their specific roles. This includes distinguishing between the early arrival of GTPase RABA2a labeled cytokinetic vesicles and the vesicle fusion mechanisms visualized by the cytokinesis-specific SNARE protein KNOLLE [2]. The removal of excess membrane material, facilitated by clathrin-coated vesicles, accompanies callose deposition. Endosidin-7 treatment reduces the amount of these vesicles, suggesting that the cell plate does not reach the excess membrane removal stage and supports the notion of a vital role for the temporal calose integration during cell plate maturation [2]. In our earlier studies in arabidopsis, we showed that endosidin-7 indirectly inhibits callose synthase activity, specifically incorporating UDP-glucose into β-1,3-glucan. Notably, the effect of endosidin-7 is specific, with no discernable differences during interphase cells in non-dividing cells. In addition, it does not affect wound-induced callose deposition or plug formation in sieve elements [2]. Consistent effects of endosidin-7 across the plant kingdom, from early diverging algae, e.g., Charophyte *Penium margaritaceum*, to higher plants, demonstrate that the pathways affected by endosidin-7 are evolutionarily conserved [9].

Arabidopsis thaliana L. (Heynh). is a well-established model organism employed in many studies to understand biological functions across the plant kingdom [10]. Many detailed omics studies have been carried out to map and investigate the transcriptome, proteome, and metabolome of arabidopsis during growth and development [11–13]. This combined wealth of arabidopsis knowledge makes this model plant an excellent choice for untargeted metabolite analysis. The significance of arabidopsis as a model system has led to several nuclear magnetic resonance (NMR)-based metabolomics studies with both solution and solid-state samples [14–17]. Recently developed approaches of ^{1}H high-resolution magic angle spinning NMR, which are circumventing the need for elaborate sample preparation and allowing utilization of solid-state NMR spectroscopy, were employed for the study of intact arabidopsis leaves [18, 19]. NMR-based methods for studying plant metabolomics, including sample preparation protocols and data analysis approaches, are being refined continuously [20, 21], contributing to a proliferation in their utilization.

In order to understand the effect of endosidin-7 on overall plant physiology and metabolism, we performed an NMR-based metabolomics analysis. Given the metabolic differences
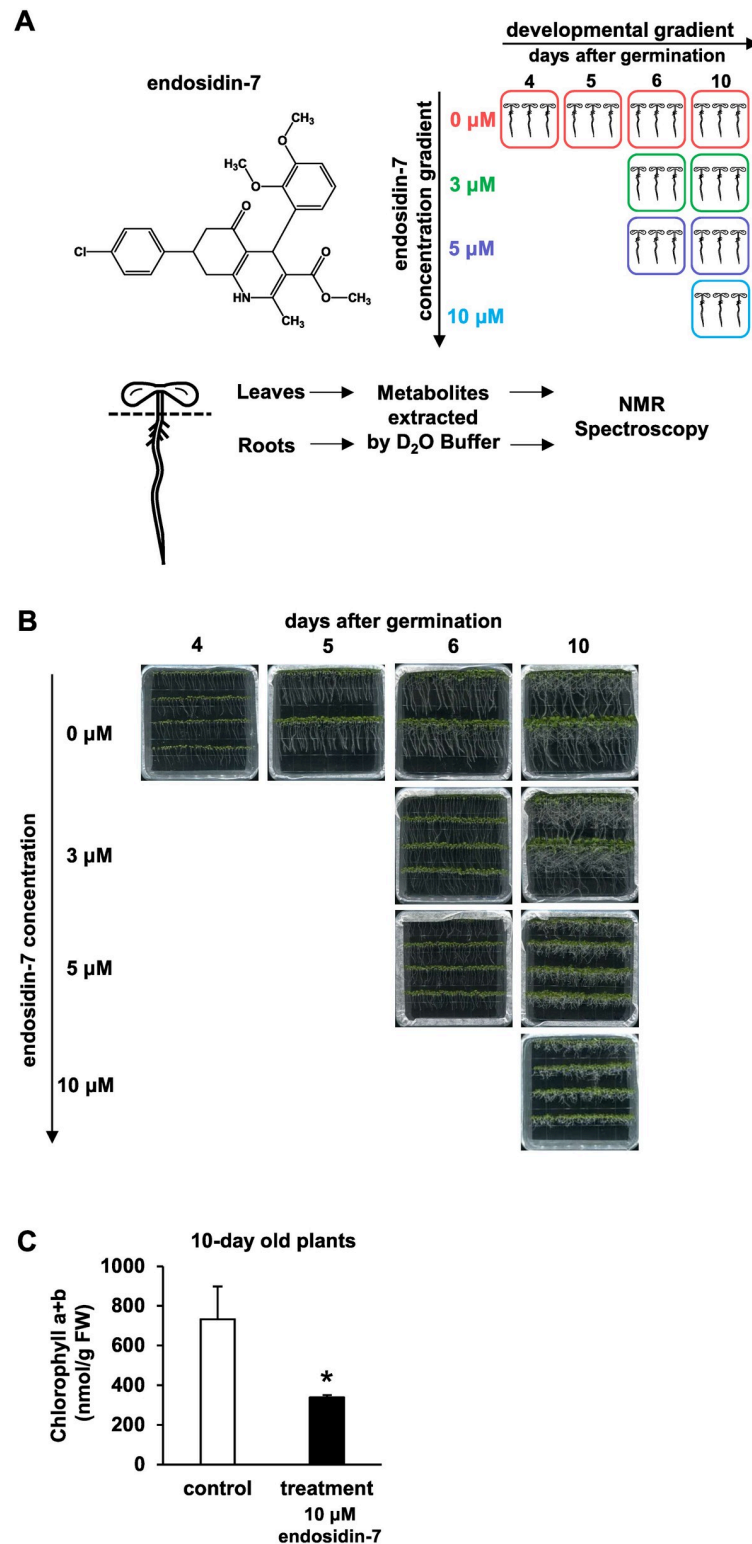
Fig 1. Experimental design and phenotypic responses to endosidin-7 treatments. (A) Experimental design of endosidin-7 treatment and NMR Metabolomics analysis. The molecular structure of endosidin-7 is shown on the left. Arabidopsis seedlings were treated with 0, 3, 5, and 10 μM of endosidin-7 and grown for up to 10-day old, with 4, 5, 6, 10-day old seedlings used as developmental controls. The cartoon of three seedlings represents three biological replicates; each replicate comprised pooled seedlings from one plate. Leaves and roots were extracted by deuterated

water and subjected to NMR spectroscopy analysis. (B) Morphological phenotype of endosidin-7 treated arabidopsis seedlings. Images were recorded before the metabolite extraction for NMR analysis. An endosidin-7 concentration-dependent inhibition of seedling growth was shown. (C) Chlorophyll content of endosidin-7 treated leaves. Samples from endosidin-7 treated leaves (10-day old) compared with the control (10-day old). A significant reduction in the chlorophyll content of endosidin-7 treated leaves was observed. Data represent the mean ± SD (n = 4), with the asterisk indicating $p < 0.05$ in the t-test.

https://doi.org/10.1371/journal.pone.0241627.g001

between aerial tissues and roots, including photosynthesis, carbon assimilation, and nutrient acquisition [22–24], we investigated roots and leaves separately. Metabolites were monitored in roots and leaves of treated and non-treated arabidopsis seedlings over periods of 4–10 days. To investigate the factors affecting metabolite levels in roots and leaves upon endosidin-7 treatment, we utilized a partial least squares discriminant analysis (PLS-DA) for the classification of metabolites across developmental stages and endosidin-7 treatment concentrations. A comprehensive multivariate statistical analysis was employed to identify and quantify the metabolites differentially altered due to endosidin-7 treatment. We found that the concentrations of over 50 metabolites were affected in arabidopsis roots and leaves as a result of endosidin-7 induced cytokinesis inhibition. Additionally, our work provides an NMR-based metabolomics protocol to study the effect of small molecules on plant metabolism.

Materials and methods

Plant materials and metabolite extraction

Arabidopsis seedlings (Columbia) were germinated on agar media with half-strength MS basal salts and 1% sucrose. Seedlings were grown at 22˚C with a 16h light cycle at ~80 µmol m^{-2} s^{-1} light intensity. Endosidin-7 was dissolved in DMSO and supplemented into the medium at concentrations of 0, 3, 5, and 10 µM. Seedlings were germinated in a vertical orientation, encouraging directional root growth, easier treatment assessment, and tissue collection. During sample harvesting, roots and leaves, including hypocotyls as indicated in **Fig 1A**, were separated by sectioning with razor blades. Metabolites were extracted following a standard procedure [20, 25]. All seedlings in one plate composed an individual biological replicate. Approximately 50 mg of root tissue and 300 mg of leaf tissue were harvested for each biological replicate. Tissue was homogenized with mortar and pestle in liquid nitrogen, and metabolites were extracted in methanol. Homogenized tissue was lysed using ice-cold 80/20 (v/v) methanol/water by v/w ratio of 3:1 in 1.5 mL tubes by vortexing/trituration and then incubated for 20 minutes on ice. Samples were centrifuged for 10 minutes at 10,000*g*, the clarified supernatant was dried in a speed-vacuum/lyophilizer, and the dried pellet was stored at -80˚C. Subsequent sample preparation for NMR spectroscopy was performed on the dried samples, as described below.

For chlorophyll quantification in leaves, 10-day old seedlings, grown as described above, were used. The glucanase activity assay was performed using leaf crude extracts of 10-day old plants. Both chlorophyll and glucanase activity analyses are described below.

Proton nuclear magnetic resonance spectroscopy

For the ^{1}H NMR analysis, the aforementioned extracted samples were resuspended to a final volume of 600 µL in D$_2$O, with 0.35 mM sodium trimethylsilyl-2,2,3,3-d$_4$-propionate (TSP) added to each lyophilized, titrated extract for chemical shift calibration. All sample preparations were performed over two days, and samples were subsequently stored at 4˚C. Quantitative ^{1}H-NMR spectra were recorded at 800 MHz and 300 K on an Avance III spectrometer (Bruker Biospin, Wissembourg, France) using a 5-mm ATMA broadband inverse probe. One-

dimensional ^{1}H experiments, with a mild pre-saturation of water resonance, were performed with a 90˚ pulse angle. NMR spectra were collected over 512 transients, with an acquisition time of 2.5 s, and a relaxation delay of 1.0 s.

The spectra were processed and analyzed with Chenomx NMR Suite 8.1 software (Chenomx Inc., 2014). Fourier-transformed spectra were multiplied with an exponential weighting function corresponding to a line-broadening of 0.5 Hz. All the spectra were manually phase-corrected, baseline optimized, and their chemical shifts were referenced to TSP. The resulted spectra were analyzed using the PROFILER-Module of Chenomx, and the concentrations of selected metabolites were estimated in all the samples. The combined concentration data was used for the multivariate statistical analysis. The metabolite peaks of the processed spectra were analyzed and assigned to their chemical shifts using the built-in Chenomx and the Human Metabolome Database [26]. The assigned metabolites were compared and confirmed through chemical shift values of other NMR based metabolomics studies performed in arabidopsis [16, 18, 27] and through comparison with the Metabolomic Repository Bordeaux (MeRy-B) database [28]. The concentrations of the assigned metabolites were determined using the Chenomx software and the concentration of the internal standard TSP [16]. All the NMR spectral data were deposited in Metabolomics Workbench (accession ST001478) under project DOI: 10.21228/M85T2G.

Statistical analysis of NMR spectroscopy datasets

Metabolite concentrations in leaf and root extracts from different experimental conditions were analyzed using multivariate statistical analyses based on previously established methods [29, 30]. A description for calculating the differential expression of metabolites between two groups can be found in the detailed protocol by Chong et al. [31]. Briefly, a linear model fit was determined for each analyte using the LIMMA package in R [32]. Lists of metabolites with the most evident differential levels between the groups (control vs. treatment; leaves vs. roots; growth periods and endosidin-7 concentration) were obtained. Significantly changed metabolites were selected via a two-step process. First, the initial data set consisted of all the metabolites for which a signal was detected for at least one feature (e.g., control group of 4-day old plants) for one condition. Second, the data from all the comparisons were combined into a single data set. The resulting combined data set consisted of metabolites exhibiting modulation for at least one experimental comparison tested. Differential measurements within groups of samples, i.e., control samples at a particular day and endosidin-7 treatment, were detected by an F-test. P-values for different analytes were transformed to compensate for multiple comparisons using the False Discovery Rate (FDR) adjustment (FC > 1.5 and p-value < 0.05) for multiple comparisons using the Benjamini-Hochberg procedure [33, 34]. Fold changes were derived from multivariate statistical analysis. This analysis allowed a comparison between multiple groups, and to provide a more meaningful value for fold change and adjusted p-values across multiple comparisons. The threshold for significance was a p-value < 0.05 for all tests with a fold change of (log2) > 1.5, unless otherwise stated in the specific analysis. All the analyses and plots were produced using a combination of Bioconductor and R [32, 35].

Spectrophotometric assays

Glucanase activity assays were performed according to the protocol provided by Choudhury [36]. Leaves of 10-day old arabidopsis seedlings grown on agar plates were homogenized in liquid nitrogen with 50 mM sodium acetate buffer (pH5.2) containing 1 mM PMSF in a 1:1 w/v ratio using mortar and pestle. The homogenates were then filtered through Miracloth (MilliporeSigma, Burlington, MA, USA), and subsequently cleared by centrifugation at 1000g for 2

min at 4˚C. The clear upper phase of the lysate was desalted by size exclusion chromatography, using a PD MiniTrap G-25 prepacked column (GE Healthcare, Chicago, IL, USA) with assay buffer as eluent. The protein content was measured by Bradford protein assay [37], and extracted proteins were used for the glucanase assay with background level estimation, as described below. A 100 μL assay mixture contained 50 μL desalted crude extract, 1 μL of DMSO or DMSO containing endosidin-7, 19 μL of DI water, and 30 μL laminarin (TCI America, Portland, OR, USA) to yield a final concentration of 15 g/L as substrate. The standard curve was established with 3.125 to 100 μg of glucose dissolved in the assay buffer. Assays were performed at 50˚C for 45 min, and terminated with 900 μL 3,5-dinitrosalicylic acid reagent at 85˚C for 10 min. Then absorbance was recorded at 510 nm on a spectrophotometer (UV-1700, Shimadzu, Kyoto, Japan). Background levels of reduced sugars in the assay were determined using boiled protein extracts as reference.

Leaf chlorophyll content was quantified according to an established protocol [38]. Briefly, chlorophyll was extracted from weighed arabidopsis leaves (20–40 mg) with 400 μL methanol/chloroform (2:1, v/v) for 1 h. Then 300 μL of water with 125 μL chloroform were added into the mixture to facilitate phase separation. After centrifugation at 10000 g for 5 min, the lower chloroform phase was air-dried and resuspended in methanol. Chlorophyll (a and b) content was calculated from the sample's absorbance at 665nm, 652 nm, and 750 nm, using the extinction coefficient for suspension in methanol and the formula provided by Porra et al. [38].

Results

Phenotypic responses of endosidin-7 treated arabidopsis seedlings

Arabidopsis seedlings were grown for 4, 5, 6, and 10 days after germination with 0 μM endosidin-7 in the media and only DMSO as reference and control (**Fig 1A and 1B**). The effect of endosidin-7 was assessed by seedling growth inhibition under 3, 5, or 10 μM endosidin-7 treatment for up to 6 or 10 days (**Fig 1A and 1B**). The selected endosidin-7 concentration range was based on the previously established (by root growth inhibition) IC_{50} of 5 μM [2]. Compared to untreated controls, endosidin-7 treated seedlings exhibited, in a concentration-dependent manner, consistently shorter roots (**Fig 1B**), corroborating our earlier observations [2]. Notably, loss of gravitropism was observed in endosidin-7 treated 10-day old samples. The aerial part of the leaves was similarly affected, as indicated by its diminished growth. To assess the impact on the leaves, we measured the chlorophyll content of 10-day old seedlings treated with 10 μM endosidin-7. The leaf chlorophyll content showed a >50% reduction compared to the untreated control (**Fig 1C**), indicating a significant loss of photosynthetic activity. Given that endosidin-7 reduces plant growth, we allowed the plants to grow for 6 or 10 days to ensure the availability of sufficient harvestable material for metabolite analysis. Metabolites were extracted from leaves and roots, and NMR spectra were recorded.

The effect of endosidin-7 treatment is greater than the developmental impact on the arabidopsis metabolomes

Generally, a difference in the NMR spectra representing the metabolite profiles was observed for the different organs, as shown by spectral excerpts of 10-day old seedlings (**S1 Fig**). A partial least squares discriminant analysis (PLS-DA) of all the untreated leaf and root samples (**S2A Fig**) underscores the prominent difference between leaf and root metabolites. Biological triplicates of control metabolomes for each time point were tightly correlated, demonstrating the consistency in the experiments and the robustness of the analysis (**S2B Fig**). In general, the NMR spectra of the leaves, in comparison with that of the roots, tend to have additional

spectral features at the aromatic region and beyond (>7.00 ppm) (**S1 Fig**). Furthermore, considering all the untreated samples (all developmental stages), the metabolites of root samples cluster much tighter than that of leaves (**S2A Fig**), indicating a larger variation in the leaf samples. PLS-DA on the different developmental control metabolomes indicated a difference across the different developmental stages (**S2C Fig**, PC1 = 16.8% and 18.8% for leaves and roots, respectively).

A multivariate analysis was performed to quantify potential changes in the observed metabolites across the developmental gradient between 4–10 days after germination. The developmental data (leaves or roots) without endosidin-7 treatment at 10, 6, 5-day old samples was compared with reference to the data of 4-day old samples. A trend of potential differences was observed, and some of the metabolites passed the fold-change criteria (> 1.5); however, the changes were not statistically significant (*p*-value > 0.05). Potentially the dense population of seedlings, especially at 10 days after germination, as shown in **Fig 1B**, could account for an increase of stress-related metabolites compared to the 4-day old plants. However, the absence of statistical differences at these stages suggests that pressure under the growth conditions did not induce discernable differences in the analyzed NMR metabolome.

A series of statistical analyses were applied to determine if the endosidin-7 treatment is the dominant factor contributing to the metabolite changes. In order to assess the degree of dispersion in the metabolomes across the developmental gradient and endosidin-7 treatment, we analyzed the metabolite data of all 27 samples (**Fig 1A**) for roots and leaves by PLS-DA. For both roots and leaves, PLS-DA for 0, 3, 5, and 10 μM endosidin-7 treatment were grouped tightly into areas of 95% confidence regions, marked by ellipses, and are well separated from the collective metabolome of the 12 untreated controls, across all developmental stages combined (**Fig 2A**). Even at the lowest used endosidin-7 concentration of 3 μM, no cluster overlap was observed with the control samples (**Fig 2A**, PC1 = 8.3% and 13.8% for leaves and roots, respectively). This shows that the plant growth under tissue culture settings and the developmental stage did not induce significant changes to mask the effect of endosidin-7. For the 10-day old plants metabolomes (**Fig 2B**), for 0, 3, 5, and 10 μM endosidin-7 concentrations, a clear separation of clusters was observed, accounting for the increased chemical treatment. The cross-validation of all the performed PLS-DA analysis, **S3 Fig**, with the corresponding unsupervised principal component analysis (PCA) **S4 Fig**, is detailed in the supporting information.

To determine if the developmental gradient has a confounding impact on the inhibitor effects, multivariate analyses were performed for a given age of plants (6 or 10-day old) and as a function of endosidin-7 concentration. The criteria for significance were defined by relative changes in the leaves or roots, in 6-day old plants (two concentrations of endosidin-7; 3 or 5 μM) or 10-day old plants (three concentrations of endosidin-7; 3, 5, or 10 μM) to the plants of the same growth stage without treatment control. For conditions (FC > 1.5 and p-value < 0.05), the analysis identified three metabolites (dimethylamine, glycerone and syringate), and with a reduced p-value to 0.1 identified six additional metabolites. Taking together, these multivariate analysis results unequivocally demonstrate that the metabolic differences between samples are primarily caused by treatment with different endosidin-7 concentrations rather than the developmental gradient of the sample.

Endosidin-7 induces changes in the primary arabidopsis metabolism

After verifying that endosidin-7 treatment caused significant changes in the metabolome composition, surpassing that of the developmental gradient, we focused on identifying the most prominently altered metabolites. In order to increase the metabolite detection sensitivity
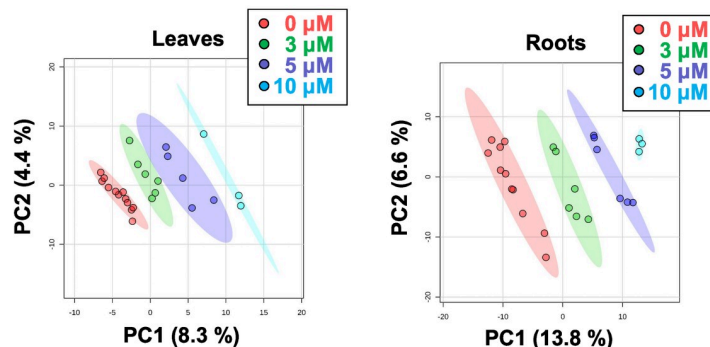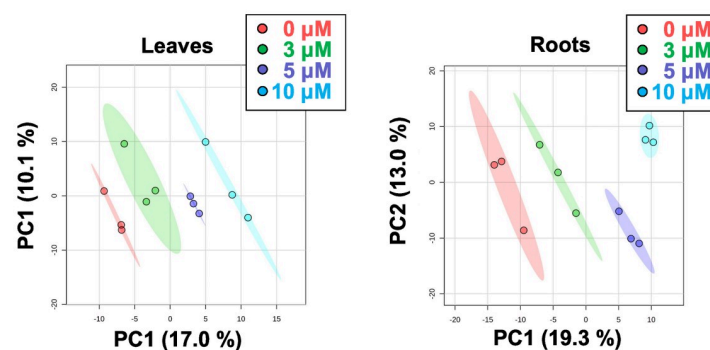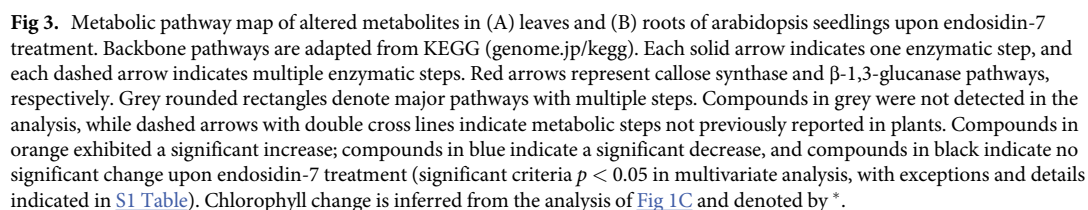
A   **PLS-DA analysis on samples of all DAGs and ES7 concentrations**

B   **PLS-DA analysis on 10 DAG samples**

Fig 2. Classification of NMR based metabolomics of the endosidin-7 treated seedlings. (A) PLS-DA analysis of all NMR data. (B) PLS-DA analysis of 10-day old samples. In (A) and (B), each dot represents one biological replicate, as indicated in Fig 1A with the same color scheme. Ellipses, indicating a 95% confidence region, are shown for the classifications of biological replicates with their respective endosidin-7 concentrations.

https://doi.org/10.1371/journal.pone.0241627.g002

within the biomarker window and the statistical power of biological replicates, we focused on comparing the endosidin-7 effect between treated and untreated samples in the leaves or roots, independent of the developmental stage. Metabolite changes were considered significant when a threshold of fold-change (log2) > 1.5 with a corresponding adjusted p-value < 0.05 was observed. A larger number of metabolites (> 100) was identified by Chemonex, however relevant plant metabolites were only considered if they can be found in the spectra of all endosidin-7 treated samples versus the control samples. The presence of fifty-three metabolites was significantly changed upon endosidin-7 treatment in leaves or roots (p < 0.05), as listed in the S1 Table (endosidin-7 treatment n = 15, control n = 12).

Individual compounds, shown in S1 Table, were first explored for their roles in arabidopsis metabolic pathways using the Kyoto Encyclopedia of Genes and Genomes (KEGG, genome.jp/kegg, [39]). Their putative involvement and role in the biochemical pathways of leaves and roots are summarized in a network map adapted from KEGG pathways, Fig 3. Detected metabolites can be categorized into components and derivatives of seven major metabolic pathways, including carbohydrate metabolism [40], glycolysis and Krebs cycle [41, 42], glycerophospholipid metabolism, branched-chain amino acid metabolism [43], glycine, serine, and arginine metabolism [44, 45], shikimate pathway [46], and the pentose phosphate pathway

Fig 3. Metabolic pathway map of altered metabolites in (A) leaves and (B) roots of arabidopsis seedlings upon endosidin-7 treatment. Backbone pathways are adapted from KEGG (genome.jp/kegg). Each solid arrow indicates one enzymatic step, and each dashed arrow indicates multiple enzymatic steps. Red arrows represent callose synthase and β-1,3-glucanase pathways, respectively. Grey rounded rectangles denote major pathways with multiple steps. Compounds in grey were not detected in the analysis, while dashed arrows with double cross lines indicate metabolic steps not previously reported in plants. Compounds in orange exhibited a significant increase; compounds in blue indicate a significant decrease, and compounds in black indicate no significant change upon endosidin-7 treatment (significant criteria $p < 0.05$ in multivariate analysis, with exceptions and details indicated in S1 Table). Chlorophyll change is inferred from the analysis of Fig 1C and denoted by *.

https://doi.org/10.1371/journal.pone.0241627.g003

[47], **S1 Table**. The average concentrations of the metabolites in the control or endosidin-7 treatment are listed for leaves and roots (**S2 Table**). Individual biological replicates are shown in the boxplot to indicate the variation of each of the metabolites in the treatment (**Fig 4**). Most of the detected metabolites are regarded as part of primary metabolism (**Fig 4A–4G**) and are involved in central plant growth and developmental processes.

Four metabolites with uncharacterized biosynthetic pathways were identified: methylguanidine, dimethylamine, trimethylamine, and acetylsalicylate. These metabolites were plotted in the metabolite map based on structural similarity with putative precursors, indicated by lozenge symbol (◊), and linked with putative precursors by dashed lines with a break in the arrows (**Fig 3**). Methylguanidine and trimethylamine have been independently reported in plant metabolomes using NMR spectroscopy [48] and liquid chromatography-tandem mass spectrometry [49].

The levels of the 53 compounds (**S1 Table**) are also shown across the different developmental stages in untreated samples and are listed in the **S3 Table**. According to the aforementioned multivariate analysis, none of these compounds showed significant changes across the observed developmental gradient in either roots or leaves. Apart from primary metabolism compounds, there were very few specialized metabolites detected, likely because they are generally of low abundance in arabidopsis and thus challenging to identify by 1D NMR profiling.

The dominant part of the modulated root metabolites showed an increase upon endosidin-7 treatment (**Fig 3B**), contrasting a decrease in leaves (**Fig 3A**). This likely reflects the difference in metabolic needs and compensatory mechanisms in aerial tissues and roots. The levels of most reduced sugars and their derivatives showed increased accumulation in roots and reduced leaves upon endosidin-7 treatment. Maltose and sucrose were exceptions, showing a decreased accumulation in roots (**Fig 4A** and **S2 Table**). A physiological concentration of maltose is known to maintain membrane potential and protect the photosynthetic electron transport chain *in vitro* [50]. The decrease of maltose in both roots and leaves upon endosidin-7 treatment may indicate a disrupted primary metabolism. In roots, endosidin-7 induced an increase of compounds upstream of the polyamine biosynthesis, including creatine, guanidinoacetate, and sarcosine (**Fig 4E**), which are derivatives of glycine, serine, and arginine. In addition, endosidin-7 treated roots exhibited an increase in 4-aminobutyrate (GABA) (**Fig 4B**), a Krebs cycle derivative., whose production is closely related to *in vivo* polyamine levels under stress [51, 52]. Endosidin-7 also modulated levels of ferulate, syringate, 5-hydroxyindole-3-acetate, and xanthurenate in both roots and leaves (**Fig 4F**). As products of the shikimate pathway, these compounds are phenylpropanoid and tryptophan derivatives related to the precursors for the biosynthesis of plant hormones, including auxin and salicylic acid [53, 54]. Taken together, these metabolite changes suggest a pronounced effect of endosidin-7 on plant hormone biosynthesis pathways.

The pool of UDP-glucose and glucose are not significantly affected by endosidin-7

We did not detect significant changes in the direct metabolic substrate and degradation product of callose (β-1,3-glucan), namely UDP-glucose and glucose, upon endosidin-7 treatment (**Fig 3**). This shows that inhibition of cytokinesis-specific callose deposition does not cause a global change in the precursor pool. Given that UDP-glucose is involved in many metabolic activities and various cell wall polysaccharide biosynthetic steps, such as starch and cellulose, the modulation of the transient accumulation of callose at the cell plate might not be discernable.

Callose deposition is regulated by the activity of both callose synthases and β-1,3-glucanases (**Fig 5A**) [55]. Arabidopsis contains twelve homologs of callose synthases [56] and fifty
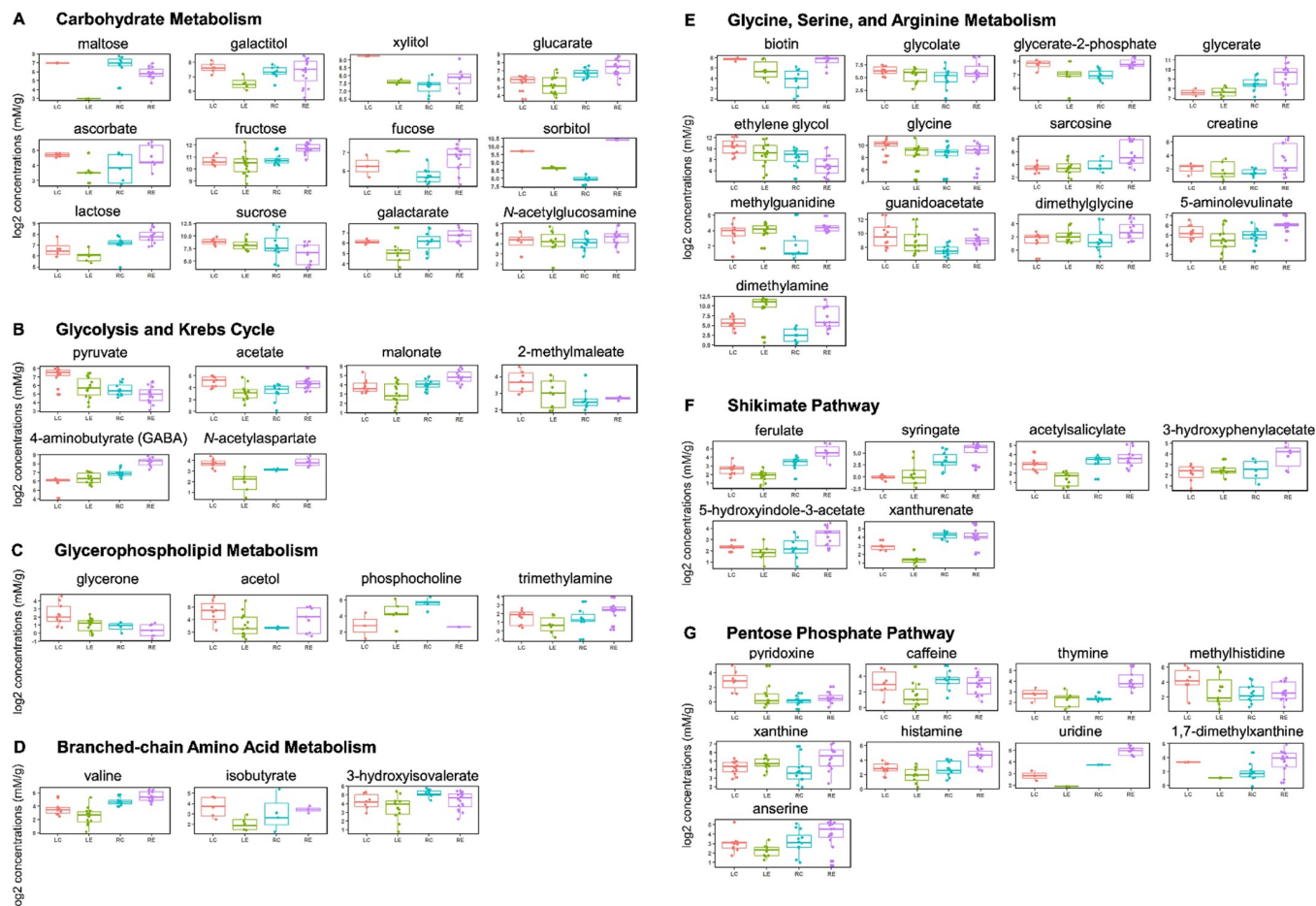
Fig 4. Differential levels of NMR detected metabolites in roots and leaves under endosidin-7. Metabolites were categorized according to their involvement in major or upstream pathways. Each panel lists a specific metabolite for LC (Control leaves, n = 12), LE (endosidin-7 treated leaves, n = 15), RC (Control roots, n = 12) and RE (endosidin-7 treated root, n = 15). Concentrations are expressed in mM/g (log2) with reference to the internal standard TSP.

homologs of β-1,3-glucanases [57]. It is plausible that endosidin-7 enhances the activity of cytokinetic β-1,3-glucanase(s), leading to higher phragmoplast callose degradation, thereby constraining polymer availability. To test this hypothesis, we examined the total glucanase activity modulation in arabidopsis crude extracts upon treatment with endosidin-7. At 10 μM and 100 μM endosidin-7, total glucanase activity did not show a statistically significant change compared to the DMSO control (**Fig 5B**). This strongly suggests that global β-1,3-glucanase activity is not affected by endosidin-7, corroborating our NMR observations that endosidin-7 does not cause a significant change in the direct metabolic substrate and degradation product of callose.

Discussion

NMR-based investigation reveals small molecule induced metabolomics changes

Plant metabolomics can be defined as the quantitative measurement of the time-related multi-parametric metabolic response of plants to environmental stimuli or genetic modification. The
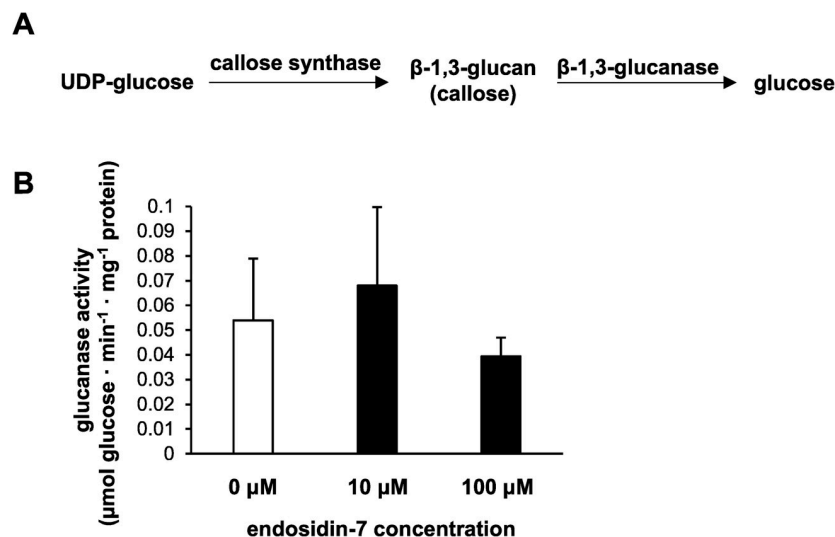
A

$$\text{UDP-glucose} \xrightarrow{\text{callose synthase}} \begin{array}{c} \beta\text{-1,3-glucan} \\ \text{(callose)} \end{array} \xrightarrow{\beta\text{-1,3-glucanase}} \text{glucose}$$

B

Fig 5. Endosidin-7 treatment does not affect glucanase activity. (A) Callose synthase and β-1,3-glucanase regulate the dynamic equilibrium of the callose deposition *in vivo*. (B) Glucanase activity in crude extracts of arabidopsis seedling leaves. Activities are measured via the amount of glucose generated by the incubation of desalted crude extracts with laminarin. No statistical difference was observed on the glucanase activity between the three treatments of DMSO, 10 μM endosidin-7, or 100 μM endosidin-7. Data are presenting the mean ± SD (n = 4).

metabolomic information content complements the genomic and proteomic approaches toward the interpretation of biological mechanisms and their function [58, 59]. Transcriptome and proteome analyses have been extensively recruited to study how organ-specific responses are coordinated during growth and are assisting a better understanding of plant development [60–64]. Considerable strides have been made in recent analytical and methodological advances, especially in the field of gene expression analysis, that now allow single-cell level-based studies. These, in turn, can unravel how gene networks are organized and regulated at the cellular level [65–67].

In the field of metabolomics, attempts to describe the metabolome of single cells have been based on tandem mass spectrometry [68]. In pioneering, spatial resolution improving work, a survey of the subcellular distribution of metabolites in cytosolic, vacuolar, and plastid fractions of arabidopsis leaves was performed by Krueger and colleagues using GC-TOF/MS and LC/MS. The results provided a topological metabolite map and took initial steps toward analyzing the metabolic dynamics between subcellular compartments [69].

While a metabolomic analysis can be performed using several mass spectrometry-based analytical chemistry techniques, NMR spectroscopy-based metabolomics analysis has some distinct advantages [70, 71]. These include easy and rapid sample preparation, elimination of derivatization analysis, which in turn allows high-throughput and quantitative analysis with a single internal standard [72–74]. In plant biology, NMR techniques have been utilized mostly for the characterization of cell wall polymers [17, 75–77]. However, the most current applications of NMR-based metabolomics in plants emphasize analytical data accumulation and sample classification, not developing 1H NMR spectroscopy as a tool to study metabolic networks [78]. This bias might be attributable to the limited availability of open-access NMR spectral libraries for plant metabolites [79, 80]. NMR studies on the whole plants have been conducted to evaluate the response of the plant defense inducer benzothiadiazole [81], the hormone methyl jasmonate involved in various signaling pathways, including tissue wound response [27], the trafficking inhibitor Sortin 1 [25], and the fungal pathogen *Verticillium dahliae* [82]. The arabidopsis

metabolic profiles, with and without pharmacological inhibition, presented here can contribute to an enhanced understanding of general plant responses to small-molecule stimuli.

Leaf and root metabolome modulations to dissect small molecule induced plant responses

We analyzed, through ^{1}H NMR spectroscopy profiling, arabidopsis leaf and root metabolites responding to the small molecule endosidin-7. Leaves and roots reacted distinctly different, clearly demonstrating organ-specific responses to endosidin-7, which could be quantified via multivariate analysis (**Fig 4** and **S2 Table**). Metabolomics has been utilized earlier to study plant abiotic or biotic stress [83, 84]. Discriminating root and leaf metabolic responses were investigated through GC or LC-MS upon sublethal cadmium exposure and high salt and low potassium stress. Principal component analysis (PCA) in these three independent metabolomics studies consistently indicated differential responses in root and leaf tissue of arabidopsis and barley [85–87]. In addition to the studies mentioned above, Novák et al. studied the organ-specific auxin metabolome of both roots and leaves of wild type and auxin over-producing arabidopsis lines by LC-MRM-MS [88]. PCA analysis revealed that the overproduction of auxin leads to distinct metabolome modulations, in which up- or down-regulation of the metabolites in leaves and roots does not follow a synchronized pattern [88]. Fontaine and colleagues showed in an NMR metabolomics study, using PCA on leaves, stems, and roots of *GLUTAMATE DEHYDROGE-NASE 3* mutants and wild type arabidopsis, that organ-specific metabolomics responses are taking place. These changes include amino acids, organic acids, and sugars [89]. In mold-resistant melon rootstocks (roots), and susceptible watermelon scions (aerial parts), organ-specific metabolite changes were observed via NMR upon exposure to the powdery mildew disease. Notably, the concentrations of root and leaf metabolites changed in opposite directions. The authors put forward the hypothesis that translocation of metabolites between rootstocks and scions through the vascular system is responsible for the antiparallel metabolome modulation [90].

Our observed trend of metabolite level changes in leaves and roots upon endosidin-7 treatment is also strikingly different (**Fig 3** and **S1 Table**), despite the similarity in cytokinesis arrest at the cellular level [2]. One plausible explanation of this antiparallel root and leave response is the aberrant translocation of metabolites between plant organs under endosidin-7 treatment. The levels of ferulate and syringate, both precursors of lignin biosynthesis, are affected upon endosidin-7 treatment (**Fig 3** and **S1 Table**). Aberrant lignin biosynthesis may further affect xylem development in arabidopsis seedlings [91], which in turn interferes with nutrient translocation and potentially giving rise to the antiparallel metabolome modulation in roots and leaves. Another equally plausible explanation is that intrinsic organ-specific regulation of primary metabolic pathways is not concomitant in plant organs under chemically induced stressed conditions. The cited studies above, together with our presented data, illustrate the importance of organ-specific investigations to assess the responses of plants comprehensively via NMR metabolomics.

Long term endosidin-7 treatment may induce hormonal responses in arabidopsis

Endosidin-7 inhibits specifically cytokinetic callose deposition but does not affect wounding stress-induced callose deposition or its deposition at sieve cells [2]. Given the specificity of endosidin-7 on cytokinetic callose, we performed a long-term endosidin-7 treatment for 6 and 10 days to investigate the metabolic phenotype that captures both the long-term growth inhibition and the cellular phenotype of arrested cell division. Together, the morphological phenotype of reduced growth, altered gravitropic response, and metabolite changes induced by

endosidin-7 treatment suggest a hormonal response from endosidin-7 exposure. Loss of gravitropism is a sign of possible hormonal regulation disruption, as it is regulated by crosstalk between auxin and other hormones [92, 93]. We did not observe a significant change in indole-3-acetate (auxin) levels upon endosidin-7 treatment; however, 5-hydroxyindole-3-acetate showed a significant increase in roots (**Fig 4F**). In independent plant metabolomics studies in melon, soybean, and *Isatis indigotica* [90, 94, 95], 5-hydroxyindole-3-acetate is reported to be putatively synthesized from tryptophan and it is speculated to affect auxin metabolism in plants [90, 95]. Considering the increase of xanthine and 1,7-dimethylxanthine in roots (**Figs 3 and 4G**), it is likely that downstream of the purine metabolism, cytokinins synthesized from the deoxyxylulose pathway [96, 97] are affected upon endosidin-7 treatment. The plant hormone salicylate, which is involved in both abiotic and biotic stress [98, 99], was not significantly changed, but levels of acetylsalicylate showed a 60% reduction upon endosidin-7 treatment in leaves (**Fig 4F** and **S2 Table**). Ambiguity for the identification of salicylate and acetylsalicylate in the present study is possible due to the strong similarity in the aromatic spectral region (in the range of 7–9 ppm) of these molecules. Further, components of the polyamine biosynthesis pathways are affected upon endosidin-7 treatment. Altogether, our data strongly suggest that the imbalance of certain hormone levels during prolonged treatment of endosidin-7 could lead to the induction of the global metabolite changes.

The proposed hormonal regulation is supported by previous long-term hormone treatment omics studies [100, 101]. Earlier microarray analysis revealed that 35 primary metabolism-related genes, involved in light signaling, nutrient uptake, and photosynthesis were altered in arabidopsis shoots treated with 5 μM isopentenyladenine (a synthetic cytokinin) for 4 days [100, 101]. Similarly, in another long-term cytokinin triggered study, lettuce treated by benzylaminopurine or meta-topolin for 13 days showed reduced accumulation of photosynthetic pigments and inhibition of photosystem II activity [102]. The phenotypes of endosidin-7 treated seedlings, plus the plethora of metabolite changes related to the primary metabolism (**Fig 3**) accompanying the loss of chlorophyll (**Fig 1C**), also suggest an aberrant hormonal regulation, as chlorophyll synthesis is tightly regulated by the balance of auxin and cytokinin [103, 104]. Both auxin and cytokinin are responsible for the initiation of the G1/S phase transition prior to cell division, a prerequisite for cell division through the regulation of cyclin-dependent kinases [105–108]. Further, crosstalk exists between the auxin and cytokinin biosynthetic pathways via the direct regulation of biosynthesis genes and transporters [109]. Endosidin-7 induced metabolome changes could reflect a compensatory mechanism counteracting the inhibition of cytokinesis and plant growth resulting from a cytokinin and auxin imbalance.

The effect of endosidin-7 inhibition on callose deposition at the division plate can be observed after a short two hours of pulse treatment [2]. This time frame is in line with characteristic hormonal responses, where gene expression or metabolite level changes are usually observed after a few hours of cytokinin or auxin induction [110–113]. Given that the cellular phenotype of cell plate disruption is observed after only two hours when treated with 50 μM, endosidin-7, these conditions could be used in future NMR metabolomic studies to dissect the long-term metabolite effects from the short-term.

Summary and perspectives

We performed an organ-specific NMR-based metabolomics study of arabidopsis leaves and roots at different developmental stages and treatments with various concentrations of the specific cytokinesis inhibitor endosidin-7. Metabolome analyses indicated that cytokinesis inhibition by endosidin-7 likely disrupts primary metabolism and hormonal regulation. This study provides metabolomics references for early stages of arabidopsis development, indicates

multiple metabolic pathways affected by endosidin-7, and highlights the relevance of organ or tissue-specific investigation in plants for an accurate and comprehensive assessment of plant metabolome modulations.

Our organ-specific examination highlighted the importance of spatial resolution in metabolite analysis. Given the complex interactions between metabolic pathways, future studies allowing higher spatial and temporal resolutions are essential for unmasking the different layers of interaction, particularly upon exogenous stimuli. There are various ways to envision how this complex task could be efficiently addressed through future developments, two promising ones are: a) automation through partially robotic extraction of the required substantial amounts of tissue, and b) improving the sensitivity of metabolite identification and metabolic flux analysis to reduce the required sample volumes. The use of stable isotopic enriched and multidimensional NMR metabolomics might be key for the latter [71, 114–116]. Technological advances, in combination with cell synchronization, might ultimately uncover very delicate metabolite changes during various cellular processes, including cytokinesis.

Supporting information

S1 Fig. Representative NMR spectra of roots and leaves (10-day old plants), and simulated spectra based on the metabolites that are significantly alerted due to endosidin-7 treatment.
(PDF)

S2 Fig. Statistical analyses of the arabidopsis metabolome without endosidin-7 treatment.
(A) PLS-DA analysis of leaves and root metabolomes. (B) Correlation analysis among 4, 5, 6, and 10-day old samples without endosidin-7 treatment. Triplicates of each developmental stage, ranked with the highest correlation with each other, are highlighted in a dashed square. Values in the squares represent the correlation coefficient between every two samples in the plot. The histogram shows the density estimation. The scatter plot displays the strength of the relationship. (C) PLS-DA analysis of metabolomics data of arabidopsis seedlings at different days after germination. Ellipses represent a 95% confidence region of the classification.
(PDF)

S3 Fig. Evaluation of the PLS-DA model. A 10-fold cross-validation, with three different measures, was performed. Blue bars indicate the accuracy of the model, pink bars (R^2, variations) indicate the goodness of fit, and light-blue bars (Q^2, prediction of the model) indicate the goodness of prediction. Good predictions with a high Q^2 value are marked by *. PLS-DA correspond to the figures: Figs 2A and 2B and S2C.
(PDF)

S4 Fig. PCA analysis of the data corresponding to PLS-DA analysis shown in Figs 2A and 2B and S2C. As indicated above, S2C Fig indicates analysis of metabolomics data of arabidopsis seedlings at different days after germination without chemical treatment, while Fig 2A describes PLS-DA analysis of all NMR data under different endosidin-7 concentrations. Fig 2B shows PLS-DA analysis of only 10-day old plants for different endosidin-7 concentrations. Score plots with the respective variances are shown in parenthesis.
(PDF)

S1 Table. Significantly changed leaves and root metabolites upon endosidin-7 treatment. The difference of metabolite levels in arabidopsis seedlings for endosidin-7 treatment (n = 15) versus the control (n = 12) is expressed by log2 fold change. The length of the colored bar is

proportional to the value, with decreases in blue and increases indicated in orange. A threshold of 1.5 (log2) was used in the multivariate analysis to calculate the *p*-value of significance.
(PDF)

S2 Table. Quantification of metabolite level changes upon endosidin-7 treatment in leaves and roots. Concentrations (mean±SD) are expressed in mM/g (log2) with reference to the internal standard TSP (n = 12 for controls, n = 15 for endosidin-7 treated).
(PDF)

S3 Table. Quantification of metabolite level modulations in leaves and roots during seedling development. Without endosidin-7 treatment, multivariate analysis does not show significant concentration modulations for these compounds (threshold of 1.5 (log2), $p < 0.05$). Concentrations (mean±SD) are expressed in mM/g (log2) with reference to the internal standard TSP (n = 3 for each developmental stage). N.D. denotes "not detected".
(PDF)

Acknowledgments

Author Contributions

Conceptualization: Thomas E. Wilkop, Viswanathan V. Krishnan, Georgia Drakakaki.

Data curation: Jaideep Singh, Viswanathan V. Krishnan.

Formal analysis: Thomas E. Wilkop, Minmin Wang, Florence Zakharov, Viswanathan V. Krishnan, Georgia Drakakaki.

Funding acquisition: Viswanathan V. Krishnan, Georgia Drakakaki.

Investigation: Thomas E. Wilkop, Minmin Wang, Angelo Heringer, Jaideep Singh, Viswanathan V. Krishnan, Georgia Drakakaki.

Supervision: Viswanathan V. Krishnan, Georgia Drakakaki.

Writing – original draft: Thomas E. Wilkop, Minmin Wang, Viswanathan V. Krishnan, Georgia Drakakaki.

Writing – review & editing: Thomas E. Wilkop, Minmin Wang, Viswanathan V. Krishnan, Georgia Drakakaki.

References

1. Drakakaki G, Robert S, Szatmari A-M, Brown MQ, Nagawa S, Van Damme D, et al. Clusters of bioactive compounds target dynamic endomembrane networks in vivo. Proc Natl Acad Sci. 2011; 108: 17850–17855. https://doi.org/10.1073/pnas.1108581108 PMID: 22006339

2. Park E, Díaz-Moreno SM, Davis DJ, Wilkop TE, Bulone V, Drakakaki G. Endosidin 7 specifically arrests late cytokinesis and inhibits callose biosynthesis, revealing distinct trafficking events during cell plate maturation. Plant Physiol. 2014; 165: 1019–1034. https://doi.org/10.1104/pp.114.241497 PMID: 24858949

3. Lipka E, Herrmann A, Mueller S. Mechanisms of plant cell division. Wiley Interdiscip Rev Dev Biol. 2015; 4: 391–405. https://doi.org/10.1002/wdev.186 PMID: 25809139

4. Samuels AL, Giddings TH, Staehelin LA. Cytokinesis in tobacco BY-2 and root tip cells: a new model of cell plate formation in higher plants. J Cell Biol. 1995; 130: 1345–57. https://doi.org/10.1083/jcb.130.6.1345 PMID: 7559757

5. Smertenko A, Assaad F, Baluška F, Bezanilla M, Buschmann H, Drakakaki G, et al. Plant cytokinesis: Terminology for structures and processes. Trends Cell Biol. 2017; 27: 885–894. https://doi.org/10.1016/j.tcb.2017.08.008 PMID: 28943203

6. McMichael CM, Bednarek SY. Cytoskeletal and membrane dynamics during higher plant cytokinesis. New Phytol. 2013; 197: 1039–1057. https://doi.org/10.1111/nph.12122 PMID: 23343343

7. Drakakaki G. Polysaccharide deposition during cytokinesis: Challenges and future perspectives. Plant Sci. 2015; 236: 177–184. https://doi.org/10.1016/j.plantsci.2015.03.018 PMID: 26025531

8. Davis DJ, McDowell SC, Park E, Hicks G, Wilkop TE, Drakakaki G. The RAB GTPase RABA1e localizes to the cell plate and shows distinct subcellular behavior from RABA2a under Endosidin 7 treatment. Plant Signal Behav. 2016; 11: 1–5. https://doi.org/10.4161/15592324.2014.984520 PMID: 27408949

9. Davis DJ, Wang M, Sørensen I, Rose JKC, Domozych DS, Drakakaki G. Callose deposition is essential for the completion of cytokinesis in the unicellular alga, *Penium margaritaceum*. J Cell Sci; 2020 Oct 12; 133(19):jcs249599. https://doi.org/10.1242/jcs.249599 PMID: 32895244

10. Meinke DW, Cherry JM, Dean C, Rounsley SD, Koornneef M. Arabidopsis thaliana: A model plant for genome analysis. Science. 1998; 282: 662–682. https://doi.org/10.1126/science.282.5389.662 PMID: 9784120

11. Van Norman JM, Benfey PN. Arabidopsis thaliana as a model organism in systems biology. Wiley Interdiscip Rev Syst Biol Med. 2009; 1: 372–379. https://doi.org/10.1002/wsbm.25 PMID: 20228888

12. Joyce AR, Palsson B. The model organism as a system: Integrating "omics" data sets. Nat Rev Mol Cell Biol. 2006; 7: 198–210. https://doi.org/10.1038/nrm1857 PMID: 16496022

13. Hennig L. Patterns of beauty—omics meets plant development. Trends Plant Sci. 2007; 12: 287–293. https://doi.org/10.1016/j.tplants.2007.05.002 PMID: 17580122

14. Sekiyama Y, Chikayama E, Kikuchi J. Profiling polar and semipolar plant metabolites throughout extraction processes using a combined solution-state and high-resolution magic angle spinning NMR approach. Anal Chem. 2010; 82: 1643–1652. https://doi.org/10.1021/ac9019076 PMID: 20121204

15. Kim SW, Koo BC, Kim J, Liu JR. Metabolic discrimination of sucrose starvation from Arabidopsis cell suspension by 1H NMR based metabolomics. Biotechnol Bioprocess Eng. 2007; 12: 653–661. https://doi.org/10.1007/BF02931082

16. Gromova M, Roby C. Toward Arabidopsis thaliana hydrophilic metabolome: Assessment of extraction methods and quantitative 1H NMR. Physiol Plant. 2010; 140: 111–127. https://doi.org/10.1111/j.1399-3054.2010.01387.x PMID: 20522173

17. Yuan Y, Teng Q, Zhong R, Haghighat M, Richardson EA, Ye ZH. Mutations of Arabidopsis TBL32 and TBL33 affect xylan acetylation and secondary wall deposition. PLoS One. 2016; 11: 1–24. https://doi.org/10.1371/journal.pone.0146460 PMID: 26745802

18. Augustijn D, Roy U, Van Schadewijk R, De Groot HJM, Alia A. Metabolic profiling of intact Arabidopsis thaliana leaves during circadian cycle using 1H high resolution magic angle spinning NMR. PLoS One. 2016; 11: 1–17. https://doi.org/10.1371/journal.pone.0163258 PMID: 27662620

19. Augustijn D, van Tol N, van der Zaal BJ, de Groot HJM, Alia A. High-resolution magic angle spinning NMR studies for metabolic characterization of Arabidopsis thaliana mutants with enhanced growth characteristics. PLoS One. 2018; 13: 1–15. https://doi.org/10.1371/journal.pone.0209695 PMID: 30596736

20. Kim HK, Choi YH, Verpoorte R. NMR-based metabolomic analysis of plants. Nat Protoc. 2010; 5: 536–549. https://doi.org/10.1038/nprot.2009.237 PMID: 20203669

21. Deborde C, Fontaine JX, Jacob D, Botana A, Nicaise V, Richard-Forget F, et al. Optimizing 1D 1H-NMR profiling of plant samples for high throughput analysis: extract preparation, standardization, automation and spectra processing. Metabolomics. 2019; 15: 1–12. https://doi.org/10.1007/s11306-019-1488-3 PMID: 30830443

22. Thomas BR, Rodriguez RL. Metabolite signals regulate gene expression and source/sink relations in cereal seedlings. Plant Physiol. 1994; 106: 1235–1239. https://doi.org/10.1104/pp.106.4.1235 PMID: 12232404

23. Koch KE. Carbohydrate-modulated gene expression in plants. Annu Rev Plant Physiol Plant Mol Biol. 1996; 47: 509–540. https://doi.org/10.1146/annurev.arplant.47.1.509 PMID: 15012299

24. Abramoff RZ, Finzi AC. Are above- and below-ground phenology in sync? New Phytol. 2015; 205: 1054–1061. https://doi.org/10.1111/nph.13111 PMID: 25729805

25. Orr DJ, Barding GA, Tolley CE, Hicks GR, Raikhel NV, Larive CK. 1H NMR-based metabolomics methods for chemical genomics experiments. Plant Chemical Genomics. Totowa, New Jersey: Humana Press; 2014. pp. 225–239. https://doi.org/10.1007/978-1-62703-592-7

26. Wishart DS, Feunang YD, Marcu A, Guo AC, Liang K, Vázquez-Fresno R, et al. HMDB 4.0: The human metabolome database for 2018. Nucleic Acids Res. 2018; 46: D608–D617. https://doi.org/10.1093/nar/gkx1089 PMID: 29140435

27. Hendrawati O, Yao Q, Kim HK, Linthorst HJM, Erkelens C, Lefeber AWM, et al. Metabolic differentiation of Arabidopsis treated with methyl jasmonate using nuclear magnetic resonance spectroscopy. Plant Sci. 2006; 170: 1118–1124. https://doi.org/10.1016/j.plantsci.2006.01.017

28. Deborde C, Jacob D. MeRy-B, a metabolomic database and knowledge base for exploring plant primary metabolism. Plant Metabolism. Totowa, New Jersey: Humana Press; 2014. pp. 3–16. https://doi.org/10.1007/978-1-62703-661-0

29. Krishnan V V., Ravindran R, Wun T, Luciw PA, Khan IH, Janatpour K. Multiplexed measurements of immunomodulator levels in peripheral blood of healthy subjects: Effects of analytical variables based on anticoagulants, age, and gender. Cytom Part B—Clin Cytom. 2014; 86: 426–435. https://doi.org/10.1002/cyto.b.21147 PMID: 24574151

30. Khan IH, Krishnan V V., Ziman M, Janatpour K, Wun T, Luciv PA, et al. Comparison of multiplex suspension array large-panel kits for profiling cytokines and chemokines in rheumatoid arthritis patients. Cytom Part B—Clin Cytom. 2009; 76: 159–168. https://doi.org/10.1002/cyto.b.20452 PMID: 18823005

31. Chong J, Wishart DS, Xia J. Using MetaboAnalyst 4.0 for Comprehensive and Integrative Metabolomics Data Analysis. Curr Protoc Bioinforma. 2019; 68: 1–128. https://doi.org/10.1002/cpbi.86 PMID: 31756036

32. R Core Team. R: A language and environment for statistical computing. Vienna, Austria, R Foundation for Statistical Computing. 2018.

33. Benjamini Y, Hochberg Y. Controlling the false discovery rate: A practical and powerful approach to multiple testing. J R Stat Soc Ser B. 1995; 57: 289–300. https://doi.org/10.1111/j.2517-6161.1995.tb02031.x

34. Benjamini Y, Drai D, Elmer G, Kafkafi N, Golani I. Controlling the false discovery rate in behavior genetics research. Behav Brain Res. 2001; 125: 279–284. https://doi.org/10.1016/s0166-4328(01)00297-2 PMID: 11682119

35. Gentleman RC, Carey VJ, Bates DM, Bolstad B, Dettling M, Dudoit S, et al. Bioconductor: open software development for computational biology and bioinformatics. Genome Biol. 2004;5. https://doi.org/10.1186/gb-2004-5-10-r80 PMID: 15461798

36. Choudhury SR, Roy S, Singh SK, Sengupta DN. Molecular characterization and differential expression of β-1,3-glucanase during ripening in banana fruit in response to ethylene, auxin, ABA, wounding, cold and light-dark cycles. Plant Cell Rep. 2010; 29: 813–828. https://doi.org/10.1007/s00299-010-0866-0 PMID: 20467747

37. Bradford MM. A rapid and sensitive method for the quantitation of microgram quantities of protein utilizing the principle of protein-dye binding. Anal Biochem. 1976; 72: 248–54. Available: http://www.ncbi.nlm.nih.gov/pubmed/942051 https://doi.org/10.1006/abio.1976.9999 PMID: 942051

38. Porra RJJ, Thompson W a. A, Kriedemann PEE. Determination of accurate extinction coefficients and simultaneous equations for assaying chlorophylls a and b extracted with four different solvents: verification of the concentration of chlorophyll standards by atomic absorption spectroscopy. Biochim Biophys Acta—Bioenerg. 1989; 975: 384–394. https://doi.org/10.1016/S0005-2728(89)80347-0

39. Kanehisa M, Goto S, Kawashima S, Nakaya A. The KEGG databases at GenomeNet. Nucleic Acids Res. 2002; 30: 42–46. https://doi.org/10.1093/nar/30.1.42 PMID: 11752249

40. Ruan Y-L. Sucrose metabolism: Gateway to diverse carbon use and sugar signaling. Annu Rev Plant Biol. 2014; 65: 33–67. https://doi.org/10.1146/annurev-arplant-050213-040251 PMID: 24579990

41. Plaxton WC. The organization and regulation of plant glycolysis. Annu Rev Plant Physiol Plant Mol Biol. 1996; 47: 185–214. https://doi.org/10.1146/annurev.arplant.47.1.185 PMID: 15012287

42. Sweetlove LJ, Beard KFM, Nunes-Nesi A, Fernie AR, Ratcliffe RG. Not just a circle: Flux modes in the plant TCA cycle. Trends Plant Sci. 2010; 15: 462–470. https://doi.org/10.1016/j.tplants.2010.05.006 PMID: 20554469

43. Binder S. Branched-chain amino acid metabolism in *Arabidopsis thaliana*. Arabidopsis Book. 2010; 8: 1–14. https://doi.org/10.1199/tab.0137 PMID: 22303262

44. Bourguignon J, Rebeille F, Douce R. Serine and glycine metabolism in higher plants. Plant amino acids. 1998. pp. 111–146.

45. Hildebrandt TM, Nunes Nesi A, Araújo WL, Braun HP. Amino acid catabolism in plants. Mol Plant. 2015; 8: 1563–1579. https://doi.org/10.1016/j.molp.2015.09.005 PMID: 26384576

46. Maeda H, Dudareva N. The shikimate pathway and aromatic amino acid biosynthesis in plants. Annu Rev Plant Biol. 2012; 63: 73–105. https://doi.org/10.1146/annurev-arplant-042811-105439 PMID: 22554242

47. Kruger NJ, Von Schaewen A. The oxidative pentose phosphate pathway: Structure and organisation. Curr Opin Plant Biol. 2003; 6: 236–246. https://doi.org/10.1016/s1369-5266(03)00039-6 PMID: 12753973

48. Wang XY, Li DZ, Li Q, Ma YQ, Yao JW, Huang X, et al. Metabolomic analysis reveals the relationship between AZI1 and sugar signaling in systemic acquired resistance of Arabidopsis. Plant Physiol Biochem. 2016; 107: 273–287. https://doi.org/10.1016/j.plaphy.2016.06.016 PMID: 27337039

49. Tsukaya H, Sawada Y, Oikawa A, Shiratake K, Isuzugawa K, Saito K, et al. Intraspecific comparative analyses of metabolites between diploid and tetraploid Arabidopsis thaliana and Pyrus communis. New Negatives Plant Sci. 2015; 1–2: 53–61. https://doi.org/10.1016/j.neps.2015.06.001

50. Kaplan F, Guy CL. β-Amylase induction and the protective role of maltose during temperature shock. Plant Physiol. 2004; 135: 1674–1684. https://doi.org/10.1104/pp.104.040808 PMID: 15247404

51. Zarei A, Trobacher CP, Shelp BJ. Arabidopsis aldehyde dehydrogenase 10 family members confer salt tolerance through putrescine-derived 4-aminobutyrate (GABA) production. Sci Rep. 2016;6. https://doi.org/10.1038/s41598-016-0015-2 PMID: 28442741

52. Shelp BJ, Bozzo GG, Trobacher CP, Zarei A, Deyman KL, Brikis CJ. Hypothesis/review: Contribution of putrescine to 4-aminobutyrate (GABA) production in response to abiotic stress. Plant Sci. 2012; 193–194: 130–135. https://doi.org/10.1016/j.plantsci.2012.06.001 PMID: 22794926

53. Zhao Y. Auxin Biosynthesis. Arabidopsis Book. 2014;e0173. https://doi.org/10.1199/tab.0173 PMID: 24955076

54. Dempsey DA, Vlot AC, Wildermuth MC, Klessig DF. Salicylic acid biosynthesis and metabolism. Arabidopsis Book. 2011; 9: e0156. https://doi.org/10.1199/tab.0156 PMID: 22303280

55. Levy A, Erlanger M, Rosenthal M, Epel BL. A plasmodesmata-associated β-1,3-glucanase in Arabidopsis. Plant J. 2007; 49: 669–682. https://doi.org/10.1111/j.1365-313X.2006.02986.x PMID: 17270015

56. Verma DPS, Hong Z. Plant callose synthase complexes. Plant Mol Biol. 2001; 47: 693–701. https://doi.org/10.1023/a:1013679111111 PMID: 11785931

57. Doxey AC, Yaish MWF, Moffatt BA, Griffith M, McConkey BJ. Functional divergence in the Arabidopsis β-1,3-glucanase gene family inferred by phylogenetic reconstruction of expression states. Mol Biol Evol. 2007; 24: 1045–1055. https://doi.org/10.1093/molbev/msm024 PMID: 17272678

58. Tian C, Chikayama E, Tsuboi Y, Kuromori T, Shinozaki K, Kikuchi J, et al. Top-down phenomics of Arabidopsis thaliana: Metabolic profiling by one- and two-dimensional nuclear magnetic resonance spectroscopy and transcriptome analysis of albino mutants. J Biol Chem. 2007; 282: 18532–18541. https://doi.org/10.1074/jbc.M700549200 PMID: 17468106

59. Schauer N, Fernie AR. Plant metabolomics: towards biological function and mechanism. Trends Plant Sci. 2006; 11: 508–516. https://doi.org/10.1016/j.tplants.2006.08.007 PMID: 16949327

60. Schad M, Lipton MS, Giavalisco P, Smith RD, Kehr J. Evaluation of two-dimensional electrophoresis and liquid chromatography—Tandem mass spectrometry for tissue-specific protein profiling of laser-microdissected plant samples. Electrophoresis. 2005; 26: 2729–2738. https://doi.org/10.1002/elps.200410399 PMID: 15971193

61. Wellmer F, Riechmann JL, Alves-ferreira M, Meyerowitz EM. Genome-wide analysis of spatial gene expression in Arabidopsis flowers. Plant Cell. 2012; 16: 1314–1326. https://doi.org/10.1105/tpc.021741.termination

62. Sreenivasulu N, Altschmied L, Radchuk V, Gubatz S, Wobus U, Weschke W. Transcript profiles and deduced changes of metabolic pathways in maternal and filial tissues of developing barley grains. Plant J. 2004; 37: 539–553. https://doi.org/10.1046/j.1365-313x.2003.01981.x PMID: 14756762

63. Müller K, Job C, Belghazi M, Job D, Leubner-Metzger G. Proteomics reveal tissue-specific features of the cress (Lepidium sativum L.) endosperm cap proteome and its hormone-induced changes during seed germination. Proteomics. 2010; 10: 406–416. https://doi.org/10.1002/pmic.200900548 PMID: 19943265

64. Ghatak A, Chaturvedi P, Nagler M, Roustan V, Lyon D, Bachmann G, et al. Comprehensive tissue-specific proteome analysis of drought stress responses in Pennisetum glaucum (L.) R. Br. (Pearl millet). J Proteomics. 2016; 143: 122–135. https://doi.org/10.1016/j.jprot.2016.02.032 PMID: 26944736

65. Nakazono M, Qiu F, Borsuk LA, Schnable PS. Laser-capture microdissection, a tool for the global analysis of gene expression in specific plant cell types: Identification of genes expressed differentially in epidermal cells or vascular tissues of maize. Plant Cell. 2003; 15: 583–596. https://doi.org/10.1105/tpc.008102 PMID: 12615934

66. Brandt S. Using array hybridization to monitor gene expression at the single cell level. J Exp Bot. 2002; 53: 2315–2323. https://doi.org/10.1093/jxb/erf093 PMID: 12432024

67. Karrer EE, Lincoln JE, Hogenhout S, Bennett AB, Bostock RM, Martineau B, et al. In situ isolation of mRNA from individual plant cells: Creation of cell-specific cDNA libraries. Proc Natl Acad Sci U S A. 1995; 92: 3814–3818. https://doi.org/10.1073/pnas.92.9.3814 PMID: 7731989

68. Misra BB, Assmann SM, Chen S. Plant single-cell and single-cell-type metabolomics. Trends Plant Sci. 2014; 19: 637–646. https://doi.org/10.1016/j.tplants.2014.05.005 PMID: 24946988

69. Krueger S, Giavalisco P, Krall L, Steinhauser MC, Büssis D, Usadel B, et al. A topological map of the compartmentalized Arabidopsis thaliana leaf metabolome. PLoS One. 2011;6. https://doi.org/10.1371/journal.pone.0017806 PMID: 21423574

70. Wolfender JL, Nuzillard JM, Van Der Hooft JJJ, Renault JH, Bertrand S. Accelerating metabolite identification in natural product research: Toward an ideal combination of liquid chromatography-high-resolution tandem mass spectrometry and NMR profiling, in silico databases, and chemometrics. Anal Chem. 2019; 91: 704–742. https://doi.org/10.1021/acs.analchem.8b05112 PMID: 30453740

71. Emwas AH, Roy R, McKay RT, Tenori L, Saccenti E, Nagana Gowda GA, et al. NMR spectroscopy for metabolomics research. Metabolites. 2019;9. https://doi.org/10.3390/metabo9070123 PMID: 31252628

72. Izquierdo-García JL, Villa P, Kyriazis A, Del Puerto-Nevado L, Pérez-Rial S, Rodriguez I, et al. Descriptive review of current NMR-based metabolomic data analysis packages. Prog Nucl Magn Reson Spectrosc. 2011; 59: 263–270. https://doi.org/10.1016/j.pnmrs.2011.02.001 PMID: 21920221

73. Marti G, Erb M, Boccard J, Glauser G, Doyen GR, Villard N, et al. Metabolomics reveals herbivore-induced metabolites of resistance and susceptibility in maize leaves and roots. Plant, Cell Environ. 2013; 36: 621–639. https://doi.org/10.1111/pce.12002 PMID: 22913585

74. Nagana Gowda GA, Raftery D. Recent advances in NMR-based metabolomics. Anal Chem. 2017; 89: 490–510. https://doi.org/10.1021/acs.analchem.6b04420 PMID: 28105846

75. Dick-Perez M, Wang T, Salazar A, Zabotina OA, Hong M. Multidimensional solid-state NMR studies of the structure and dynamics of pectic polysaccharides in uniformly 13C-labeled Arabidopsis primary cell walls. Magn Reson Chem. 2012; 50: 539–550. https://doi.org/10.1002/mrc.3836 PMID: 22777793

76. Phyo P, Wang T, Xiao C, Anderson CT, Hong M. Effects of pectin molecular weight changes on the structure, dynamics, and polysaccharide interactions of primary cell walls of Arabidopsis thaliana: Insights from solid-state NMR. Biomacromolecules. 2017; 18: 2937–2950. https://doi.org/10.1021/acs.biomac.7b00888 PMID: 28783321

77. Wang T, Park YB, Caporini MA, Rosay M, Zhong L, Cosgrove DJ, et al. Sensitivity-enhanced solid-state NMR detection of expansin's target in plant cell walls. Proc Natl Acad Sci U S A. 2013; 110: 16444–16449. https://doi.org/10.1073/pnas.1316290110 PMID: 24065828

78. Krishnan P, Kruger NJ, Ratcliffe RG. Metabolite fingerprinting and profiling in plants using NMR. J Exp Bot. 2005; 56: 255–265. https://doi.org/10.1093/jxb/eri010 PMID: 15520026

79. Ludwig C, Easton JM, Lodi A, Tiziani S, Manzoor SE, Southam AD, et al. Birmingham Metabolite Library: A publicly accessible database of 1-D 1H and 2-D 1H J-resolved NMR spectra of authentic metabolite standards (BML-NMR). Metabolomics. 2012; 8: 8–18. https://doi.org/10.1007/s11306-011-0347-7

80. Johnson SR, Lange BM. Open-access metabolomics databases for natural product research: Present capabilities and future potential. Front Bioeng Biotechnol. 2015; 3: 1–10. https://doi.org/10.3389/fbioe.2015.00001 PMID: 25654078

81. Hien Dao TT, Puig RC, Kim HK, Erkelens C, Lefeber AWM, Linthorst HJM, et al. Effect of benzothiadiazole on the metabolome of Arabidopsis thaliana. Plant Physiol Biochem. 2009; 47: 146–152. https://doi.org/10.1016/j.plaphy.2008.10.001 PMID: 19010687

82. Su X, Lu G, Guo H, Zhang K, Li X, Cheng H. The dynamic transcriptome and metabolomics profiling in Verticillium dahliae inoculated Arabidopsis thaliana. Sci Rep. 2018; 8: 1–11. https://doi.org/10.1038/s41598-017-17765-5 PMID: 29311619

83. Kim SG, Yon F, Gaquerel E, Gulati J, Baldwin IT. Tissue specific diurnal rhythms of metabolites and their regulation during herbivore attack in a native Tobacco, Nicotiana attenuata. PLoS One. 2011;6. https://doi.org/10.1371/journal.pone.0026214 PMID: 22028833

84. Ullah N, Yüce M, Neslihan Öztürk Gökçe Z, Budak H. Comparative metabolite profiling of drought stress in roots and leaves of seven Triticeae species. BMC Genomics. 2017; 18: 1–12. https://doi.org/10.1186/s12864-016-3406-7 PMID: 28049423

85. Keunen E, Florez-Sarasa I, Obata T, Jozefczak M, Remans T, Vangronsveld J, et al. Metabolic responses of Arabidopsis thaliana roots and leaves to sublethal cadmium exposure are differentially influenced by ALTERNATIVE OXIDASE1a. Environ Exp Bot. 2016; 124: 64–78. https://doi.org/10.1016/j.envexpbot.2015.11.015

86. Zeng J, Quan X, He X, Cai S, Ye Z, Chen G, et al. Root and leaf metabolite profiles analysis reveals the adaptive strategies to low potassium stress in barley. BMC Plant Biol. 2018; 18: 187. https://doi.org/10.1186/s12870-018-1404-4 PMID: 30200885

87. Wu D, Cai S, Chen M, Ye L, Chen Z, Zhang H, et al. Tissue metabolic responses to salt stress in wild and cultivated barley. PLoS One. 2013;8. https://doi.org/10.1371/journal.pone.0055431 PMID: 23383190

88. Novák O, Hényková E, Sairanen I, Kowalczyk M, Pospíšil T, Ljung K. Tissue-specific profiling of the Arabidopsis thaliana auxin metabolome. Plant J. 2012; 72: 523–536. https://doi.org/10.1111/j.1365-313X.2012.05085.x PMID: 22725617

89. Fontaine JX, Molinié R, Tercé-Laforgue T, Cailleu D, Hirel B, Dubois F, et al. Use of 1H-NMR metabolomics to precise the function of the third glutamate dehydrogenase gene in Arabidopsis thaliana. Comptes Rendus Chim. 2010; 13: 453–458. https://doi.org/10.1016/j.crci.2009.08.003

90. Mahmud I, Kousik C, Hassell R, Chowdhury K, Boroujerdi AF. NMR spectroscopy identifies metabolites translocated from powdery mildew resistant rootstocks to Susceptible Watermelon Scions. J Agric Food Chem. 2015; 63: 8083–8091. https://doi.org/10.1021/acs.jafc.5b02108 PMID: 26302171

91. Taylor-Teeples M, Lin L, De Lucas M, Turco G, Toal TW, Gaudinier A, et al. An Arabidopsis gene regulatory network for secondary cell wall synthesis. Nature. 2015; 517: 571–575. https://doi.org/10.1038/nature14099 PMID: 25533953

92. Nziengui H, Lasok H, Kochersperger P, Ruperti B, Rébeillé F, Palme K, et al. Root gravitropism is regulated by a crosstalk between para-aminobenzoic acid, ethylene, and auxin. Plant Physiol. 2018; 178: 1370–1389. https://doi.org/10.1104/pp.18.00126 PMID: 30275058

93. Philosoph-Hadas S, Friedman H, Meir S. Gravitropic bending and plant hormones. Vitam Horm. 2005; 72: 31–78. https://doi.org/10.1016/S0083-6729(05)72002-1 PMID: 16492468

94. Cao YW, Qu RJ, Miao YJ, Tang XQ, Zhou Y, Wang L, et al. Untargeted liquid chromatography coupled with mass spectrometry reveals metabolic changes in nitrogen-deficient Isatis indigotica Fortune. Phytochemistry. 2019; 166: 112058. https://doi.org/10.1016/j.phytochem.2019.112058 PMID: 31280093

95. feng Jiang Z, dan Liu D, qiong Wang T, long Liang X, hai Cui Y, hua Liu Z, et al. Concentration difference of auxin involved in stem development in soybean. J Integr Agric. 2020; 19: 953–964. https://doi.org/10.1016/S2095-3119(19)62676-6

96. Zrenner R, Stitt M, Sonnewald U, Boldt R. Pyrimidine and purine biosynthesis and degradation in plants. Annu Rev Plant Biol. 2006; 57: 805–836. https://doi.org/10.1146/annurev.arplant.57.032905.105421 PMID: 16669783

97. Mok DWS, Mok MC. Cytokinin metabolism and action. Annu Rev Plant Physiol. 2001; 52: 89–118. https://doi.org/10.1146/annurev.arplant.52.1.89 PMID: 11337393

98. Loake G, Grant M. Salicylic acid in plant defence-the players and protagonists. Curr Opin Plant Biol. 2007; 10: 466–472. https://doi.org/10.1016/j.pbi.2007.08.008 PMID: 17904410

99. Khan MIR, Fatma M, Per TS, Anjum NA, Khan NA. Salicylic acid-induced abiotic stress tolerance and underlying mechanisms in plants. Front Plant Sci. 2015; 6: 1–17. https://doi.org/10.3389/fpls.2015.00001 PMID: 25653664

100. Brenner WG, Ramireddy E, Heyl A, Schmülling T. Gene regulation by cytokinin in Arabidopsis. Front Plant Sci. 2012; 3: 1–22. https://doi.org/10.3389/fpls.2012.00001 PMID: 22645563

101. Che P, Gingerich DJ, Lall S, Howell SH. Global and hormone-induced gene expression changes during shoot development in Arabidopsis. Plant Cell. 2002; 14: 2771–2785. https://doi.org/10.1105/tpc.006668 PMID: 12417700

102. Prokopová J, Špundová M, Sedlářová M, Husičková A, Novotný R, Doležal K, et al. Photosynthetic responses of lettuce to downy mildew infection and cytokinin treatment. Plant Physiol Biochem. 2010; 48: 716–723. https://doi.org/10.1016/j.plaphy.2010.04.003 PMID: 20471849

103. Hudson D, Guevara D, Yaish MW, Hannam C, Long N, Clarke JD, et al. GNC and CGA1 modulate chlorophyll biosynthesis and glutamate synthase (GLU1/FD-GOGAT) expression in Arabidopsis. PLoS One. 2011;6. https://doi.org/10.1371/journal.pone.0026765 PMID: 22102866

104. Liu X, Li Y, Zhong S. Interplay between light and plant hormones in the control of arabidopsis seedling chlorophyll biosynthesis. Front Plant Sci. 2017; 8: 1–6. https://doi.org/10.3389/fpls.2017.00001 PMID: 28220127

105. Wang L, Ruan YL. Regulation of cell division and expansion by sugar and auxin signaling. Front Plant Sci. 2013; 4: 1–9. https://doi.org/10.3389/fpls.2013.00001 PMID: 23346092

106. Schaller GE, Street IH, Kieber JJ. Cytokinin and the cell cycle. Curr Opin Plant Biol. 2014; 21: 7–15. https://doi.org/10.1016/j.pbi.2014.05.015 PMID: 24994531

107. Hartig K, Beck E. Crosstalk between auxin, cytokinins, and sugars in the plant cell cycle. Plant Biol. 2006; 8: 389–396. https://doi.org/10.1055/s-2006-923797 PMID: 16807832

108. Moubayidin L, Di Mambro R, Sabatini S. Cytokinin-auxin crosstalk. Trends Plant Sci. 2009; 14: 557–562. https://doi.org/10.1016/j.tplants.2009.06.010 PMID: 19734082

109. Ruiz Rosquete M, Barbez E, Kleine-Vehn J. Cellular auxin homeostasis: Gatekeeping is housekeeping. Mol Plant. 2012; 5: 772–786. https://doi.org/10.1093/mp/ssr109 PMID: 22199236

110. Talbott LD, Ray PM. Changes in molecular size of previously deposited and newly synthesized pea cell wall matrix polysaccharides: Effects of auxin and turgor. Plant Physiol. 1992; 98: 369–379. https://doi.org/10.1104/pp.98.1.369 PMID: 16668638

111. Zürcher E, Tavor-Deslex D, Lituiev D, Enkerli K, Tarr PT, Müller B. A robust and sensitive synthetic sensor to monitor the transcriptional output of the cytokinin signaling network in planta. Plant Physiol. 2013; 161: 1066–1075. https://doi.org/10.1104/pp.112.211763 PMID: 23355633

112. Kull U, Kühn B, Schweizer J, Weiser H. Short-term effects of cytokinins on the lipid fatty acids of green leaves. Plant Cell Physiol. 1978; 19: 801–810. https://doi.org/10.1093/oxfordjournals.pcp.a075654

113. Petit-Paly G, Franck T, Brisson L, Kevers C, Chénieux JC, Rideau M. Cytokinin modulates catalase activity and coumarin accumulation in in vitro cultures of tobacco. J Plant Physiol. 1999; 155: 9–15. https://doi.org/10.1016/S0176-1617(99)80134-5

114. Deborde C, Moing A, Roch L, Jacob D, Rolin D, Giraudeau P. Plant metabolism as studied by NMR spectroscopy. Prog Nucl Magn Reson Spectrosc. 2017; 102–103: 61–97. https://doi.org/10.1016/j.pnmrs.2017.05.001 PMID: 29157494

115. Lane AN, Fan TWM. NMR-based stable isotope resolved metabolomics in systems biochemistry. Arch Biochem Biophys. 2017; 628: 123–131. https://doi.org/10.1016/j.abb.2017.02.009 PMID: 28263717

116. Markley JL, Brüschweiler R, Edison AS, Eghbalnia HR, Powers R, Raftery D, et al. The future of NMR-based metabolomics. Curr Opin Biotechnol. 2017; 43: 34–40. https://doi.org/10.1016/j.copbio.2016.08.001 PMID: 27580257